Shadow Detection with Conditional Generative Adversarial Networks

Vu Nguyen, Tomas F. Yago Vicente, Maozheng Zhao, Minh Hoai, Dimitris Samaras
Stony Brook University, Stony Brook, NY 11794, USA
{vhnguyen, tyagovicente, mazhao, minhhoai, samaras}@cs.stonybrook.edu

Abstract

We introduce scGAN, a novel extension of conditional Generative Adversarial Networks (GAN) tailored for the challenging problem of shadow detection in images. Previous methods for shadow detection focus on learning the local appearance of shadow regions, while using limited local context reasoning in the form of pairwise potentials in a Conditional Random Field. In contrast, the proposed adversarial approach is able to model higher level relationships and global scene characteristics. We train a shadow detector that corresponds to the generator of a conditional GAN, and augment its shadow accuracy by combining the typical GAN loss with a data loss term. Due to the unbalanced distribution of the shadow labels, we use weighted cross entropy. With the standard GAN architecture, properly setting the weight for the cross entropy would require training multiple GANs, a computationally expensive grid procedure. In scGAN, we introduce an additional sensitivity parameter w to the generator. The proposed approach effectively parameterizes the loss of the trained detector. The resulting shadow detector is a single network that can generate shadow maps corresponding to different sensitivity levels, obviating the need for multiple models and a costly training procedure. We evaluate our method on the large-scale SBU and UCF shadow datasets, and observe up to 17% error reduction with respect to the previous state-of-the-art method.

1. Introduction

Images contain shadows and shadows provide useful cues about the depicted scenes, from light sources [12, 22, 23, 24], object shapes [21], camera parameters and geo-location [7], and geometry [8]. Shadow detection is therefore a fundamental component of scene understanding. However, automatic shadow detection is challenging because it requires both local and global reasoning—the appearance of a shadow area depends on the material of a local surface and the global scene structure and illumination condition. Unfortunately, most existing methods for shadow detection are based on local region classification, failing to
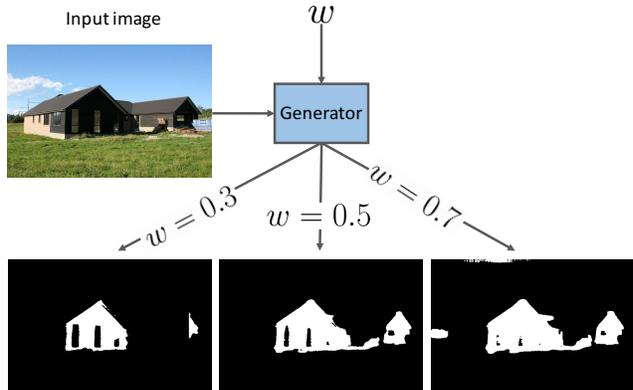
Figure 1: We propose scGAN for shadow detection. scGAN has a tunable sensitivity parameter w that regulates the amount of shadow pixels in the predicted shadow map. This figure shows scGAN with several generated shadow maps corresponding to different values of the sensitivity parameter w. A larger parameter w leads to a shadow map with a larger shadow area.

reason about the global image semantics. Some methods use Conditional Random Fields [11] as a way to incorporate pairwise contextual cues. However, this post processing approach is still local—global consistency and high order interaction between scene elements are not enforced.

In this paper, we propose a method for shadow detection based on the Conditional Generative Adversarial Network (cGAN) [20], a special type of Generative Adversarial Networks (GANs) [3]. A cGAN has two components: a discriminator and a generator. The generator can be trained to generate an output image conditioned on an input image. In our case, we will train the generator of a cGAN to produce the shadow mask given the input scene image. Unlike a local region classifier, the generator of a cGAN has a full view of the entire image and it can reason about the global structure and context. The generator is also trained to output a shadow mask that sufficiently harmonizes with the scene image; otherwise, the discriminator can easily distinguish between a generated shadow mask and a real shadow mask.

It is worth mentioning that cGANs have been successfully applied to other image-to-image translation problems, including image superresolution [15], image inpainting [25], style transfer [16], video frame prediction [19], and future prediction [31].

However, one drawback of cGANs is their inflexibility. Once a cGAN has been trained, it cannot be easily adapted to satisfy any new requirements. Particularly for shadow detection, it will be impossible to tune the sensitivity of the detector because there is no sensitivity parameter. For certain images and domains, this can be frustrating because we cannot ask the detector to output fewer or more shadow pixels. The reader might wonder whether we can simply train a cGAN to output a continuous shadow probability map instead of a binary mask. However the generator of a cGAN will always generate images that are close to binary images even though we do not enforce binary output. This is because the generator is trained to fool the discriminator, and a non-binary image can be easily classified as a fake shadow mask. The only solution would be to train multiple cGANs for different sensitivity levels and pick the best, at huge computational cost.

In this paper, we propose scGAN, a novel cGAN architecture with a tunable sensitivity parameter. An scGAN differs from a cGAN in multiple aspects: the network architecture, the loss function, and the training procedure. *i)* The generator of an scGAN has an additional input, which is the sensitivity parameter, as illustrated in Figure 1. *ii)* The training loss of the generator is augmented to include a loss term that encourages agreement between the generator's output and the corresponding ground truth target image. This loss term is based on weighted cross entropy, where the weight corresponds to the sensitivity parameter. *iii)* We propose an efficient training procedure to train the generator to respond appropriately to different sensitivity parameter values.

To evaluate our shadow detection method we perform experiments on the SBU dataset [30] which is the largest publicly available shadow dataset and on the UCF dataset [32] and observe that our proposed approach outperforms the previous state of the art [30]. In terms of balanced error rate we obtain a significant 17% and 12% error reduction on SBU and UCF respectively. Moreover, we reduce the error in shadow pixels by almost 20% (SBU) and 15% (UCF) while correctly detecting 17% (SBU) and 11 %(UCF) more non-shadow pixels with respect to [30]. This work contains the following contributions:

- We present the first application of adversarial training for shadow detection.

- We develop scGAN, a novel conditional GAN architecture with a tunable sensitivity parameter that can be efficiently trained.

- The proposed method outperforms the state-of-the-art

by a wide margin for shadow detection in the challenging SBU [30] and UCF [32] datasets.

2. Previous Work

2.1. Single image shadow detection

Single image shadow detection has been widely studied. Early work used physical models of illumination and color. These methods, such as the illumination invariant approaches of Finlayson *et al.* [1, 2], only work well on high quality images [13]. For consumer photographs and web quality images, data-driven statistical learning approaches [4, 5, 13, 28, 32] are more effective, as shown in the two benchmark shadow datasets: UCF [32] and UIUC [4]. These methods learn the appearance of shadow areas from images with annotated ground truth.

There have been great advances in shadow detection in the recent years. Khan *et al.* [9] were the first to use deep learning to automatically learn features for shadow detection that significantly improved the state of the art. First, they trained two Convolutional Neural Networks (CNNs): one CNN is trained to label shadow regions, the other CNN was trained to label shadow boundaries. Then, the predictions from both CNNs were combined into a unary potential for a CRF that labels image pixels as shadow/non-shadow. They also added to the CRF a pairwise potential with an Ising prior that penalizes different label assignments for adjacent pixels with similar intensities. Vicente *et al.* [27, 29] proposed a multikernel model for shadow region classification. The parameters and hyperparameters of the model were efficiently optimized based on least-squares SVM leave-one-out estimates. They also embedded the multikernel region classifier into a CRF with added context based pairwise potentials. Their pairwise potentials introduced more contextual cues than the simple Ising prior of Khan *et al.* [9]. However, these only model local interactions between neighboring regions of an image. More recent work of Vicente *et al.* [30] used a stacked CNN for large scale shadow detection. The stacked architecture refines the image level predictions of a FCN [17], pretrained for semantic labeling, with a patch-based CNN tuned on shadow data. This architecture achieved state-of-the-art results on several datasets. However, this approach is not end-to-end and it requires a cumbersome two step training: firstly an FCN is trained to generate the image level shadow-prior. The image level prior is then combined with RGB local patches for the later training of the patch-based CNN which produces shadow masks for the local patches. In this approach, some more global context is considered as the FCN makes image level predictions. However, the final shadow predictions are made by the patch-based CNN, which does not take into account pixels further than the width of the patch.

3. scGAN for Shadow Detection

We propose scGAN, a novel architecture that addresses the limitations of the standard cGAN approach for shadow detection, as explained in Section 3.1. This section describes the architecture, the training loss, and the training procedure of scGAN.

3.1. Conditional Generative Adversarial Networks

Generative Adversarial Networks (GANs) [3], are recently proposed generative models for images. A GAN consists of two adversarial networks: a generator G, and a discriminator D. The generator G aims to generate a realistic image, having been given as input z, a latent random vector sampled from some noise distribution. The discriminator D learns to classify if a given image was generated by G (fake sample) or it is indeed a real image from the training set. Hence, the two models compete against each other. G aims to generate images that will be hard for D to discern as fake, thus learning the data distribution from the training set. Meanwhile D aims to avoid being deceived by G.

Conditional Generative Adversarial Networks (cGANs) [20] are an extension of GANs that allows the introduction of additional observed information (conditioning variable) to both the generator (G) and the discriminator (D). For instance, a cGAN can be applied to the shadow detection task by using as conditioning variable an input RGB scene image $\mathbf{x}$. The generator G is trained to output a shadow mask $G(\mathbf{z}, \mathbf{x})$ ($\mathbf{z}$ is an random variable for GAN) that can realistically correspond to $\mathbf{y}$, the shadows depicted in the input image $\mathbf{x}$. G learns to model the distribution $p_{data}(\mathbf{x}, \mathbf{y})$ of the training data which consists of pairs of input image $\mathbf{x}$ and ground-truth shadow mask $\mathbf{y}$. Then D is presented with either $(\mathbf{x},\mathbf{y})$ or $(\mathbf{x},G(\mathbf{z}, \mathbf{x}))$ and has to decide if the pair truly comes from the training data. The objective function for the cGAN is:

$$\mathcal{L}_{cGAN}(G, D) = \mathbf{E}_{\mathbf{x},\mathbf{y}\sim p_{data}(\mathbf{x},\mathbf{y})}[\log D(\mathbf{x}, \mathbf{y})] +$$
$$\mathbf{E}_{\mathbf{x}\sim p_{data}(\mathbf{x}),\mathbf{z}\sim p_z(\mathbf{z})}[\log(1 - D(\mathbf{x}, G(\mathbf{z}, \mathbf{x})))]. \quad (1)$$

It is possible to have a deterministic generator G. This can be achieved by eliminating the random variable $\mathbf{z}$. In this case, the objective function of a cGAN can be simplified to:

$$\mathcal{L}_{cGAN}(G, D) = \mathbf{E}_{\mathbf{x},\mathbf{y}\sim p_{data}(\mathbf{x},\mathbf{y})}[\log D(\mathbf{x}, \mathbf{y})] +$$
$$\mathbf{E}_{\mathbf{x}\sim p_{data}(\mathbf{x})}[\log(1 - D(\mathbf{x}, G(\mathbf{x})))]. \quad (2)$$

Previous works [6, 18, 25] using cGANs often introduce a data loss term to encourage the generated image $G(\mathbf{x})$ to be close to the ground truth image $\mathbf{y}$, e.g.,

$$\mathcal{L}_{data}(G) = \mathbf{E}_{\mathbf{x},\mathbf{y}\sim p_{data}(\mathbf{x},\mathbf{y})}||\mathbf{y} - G(\mathbf{x})||^2. \quad (3)$$

The generator is encouraged to both fool the discriminator and produce an output that is close to the ground-truth.

Training a cGAN equates to the generator and the discriminator playing a min-max game:

$$\min_G \max_D \mathcal{L}_{cGAN}(G, D) + \lambda \mathcal{L}_{data}(G). \quad (4)$$

Conditional GANs provide an elegant framework for shadow detection. A cGAN is able to effectively enforce higher order consistencies, that cannot be modeled with CRF pairwise terms or per pixel data loss. This is thanks to the adversarial model's ability to asses the joint configuration of input image and output mask [18]. This confers an advantage to our method, compared to previous shadow detection approaches.

Shadow detection is a binary classification problem with highly unbalanced classes: typically there are significantly fewer shadow pixels than non shadow pixels in natural images. However, good performance for both classes is desired. This is often addressed by adjusting the classification threshold accordingly, and/or setting different misclassification costs for each class. Unfortunately, neither approaches can be easily applied to the standard cGAN formulation. First, because of the adversarial training, G will learn to output binary values in the shadow masks, otherwise it would be easy for the discriminator D to detect fakes (ground-truth masks are binary). Second, although $\mathcal{L}_{data}(G)$ can take the form of a per class weighted loss, properly tuning these class weights would require a grid search with models retrained over all possible weight values, potentially an extremely computational cost.

3.2. Sensitivity parameter

Compared to cGAN, scGAN has an additional sensitivity parameter w that serves two purposes, see Figure 2. First, it is an input of the generator G and it controls the sensitivity of the generator. The generator G is still conditioned on the input scene image, but a larger w will generate a predicted shadow mask with more shadow pixels and vise versa. Second, the parameter w is also a parameter of the loss function, weighting the relative importance of shadow and non-shadow classes. Formally, consider a particular pixel and suppose the ground truth value is y ($y = 1$ if this is a shadow pixel and $y = 0$ for non-shadow pixel). Suppose the generator outputs a probability value g for this pixel ($0 \leq g \leq 1$) being a shadow. The data loss for this pixel is defined as the weighted cross entropy loss:

$$-\big(wy\log(g) + (1 - w)(1 - y)\log(1 - g)\big). \quad (5)$$

This loss is $-w\log(g)$ if y is a shadow pixel and $(w - 1)\log(1-g)$ if y is a non-shadow pixel. Thus, if $w \gg 1-w$, we will penalize a wrongly classified shadow pixel much more than a wrongly classified non-shadow pixel.

Let $G(\mathbf{x}, w)$ denote the predicted shadow probability map for input image $\mathbf{x}$ at sensitivity level w. For mathematical convenience, assume $G(\mathbf{x}, w)$ is represented as a
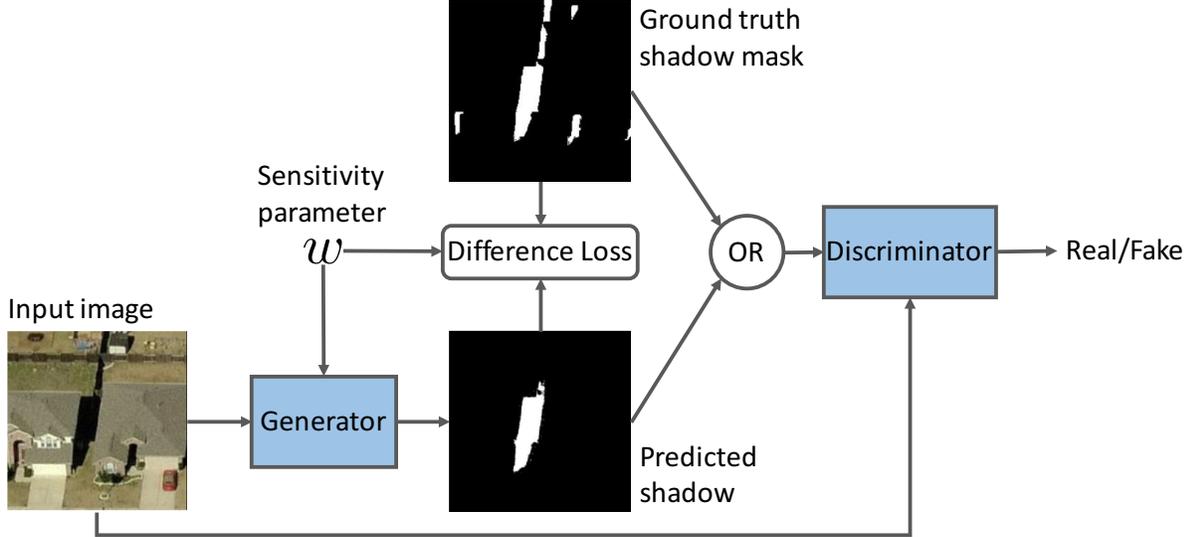
Figure 2: **scGAN for shadow detection.** The sensitivity parameter w, affects the generator loss and obviates the need for training multiple models to tune the class balance.

column vector (a vectorized image), and the ground truth shadow mask **y** is also a column vector. The data loss term for scGAN is defined as:

$$\mathcal{L}_{data}(G, w) = \mathbf{E}_{\mathbf{x}, \mathbf{y} \sim p_{data}(\mathbf{x}, \mathbf{y})}[-w\mathbf{y}^T \log(G(\mathbf{x}, w)) - (1 - w)(1 - \mathbf{y}^T) \log(1 - G(\mathbf{x}, w))]. \quad (6)$$

Finally, the objective of the scGAN is defined as:

$$\mathcal{L}_{cGAN}(G, D) + \lambda \mathbf{E}_{w \sim \mathcal{U}[0,1]}[\mathcal{L}_{data}(G, w)], \quad (7)$$

where $\mathcal{U}[0, 1]$ denotes the uniform distribution between 0 and 1. The generator and discriminator can be trained adversarially. The discriminator aims to maximize the above objective while the generator tries to minimize the objective. Once trained, we obtain a generator that is effectively a shadow detector parameterized by the sensitivity parameter w. This offers the ability to efficiently tune the sensitivity of the detector for shadow pixels without having to retrain the model.

3.3. Generator and Discriminator architectures

An scGAN has two parts, a generator and a discriminator. Both the generator and the discriminator are deep convolutional neural networks [14].

Architecture of the generator. The generator of our model is inspired by the U-Net architecture [26]. The U-Net, originally designed for image segmentation, has two parts, a convolutional net followed by a deconvolutional net. There are by-pass contracting paths connecting the layers of the convolutional net and the decovolutional net, which lead to finer segmentation and more precise localization.

Our architecture, similar to [6], has the following layers: conv64, conv_RB128, conv_RB256, conv_RB512(5 times), deconv_DR512(3 times), deconv_R512, deconv_R256, deconv_R128, deconv_R64, deconv_1, where conv denotes convolutional layer; conv_RB denotes a block of Leaky ReLU (slope 0.2), convolutional layer and batch normalization; deconv_R denotes a block of ReLU followed by a deconvolutional layer, batch normalization, and concatenation; deconv_DR is a deconv_R with an additional dropout layer right after the batch normalization; deconv denotes ReLU and deconvolutional layer followed by a $tanh$ operator. Every convolutional and deconvolutional layer has filter size of 5×5 and stride of 2. The numbers after the layer denomination correspond to the amount of filters in the corresponding convolutional or deconvolutional layer. The concatenation layer in the ith deconv block concatenates the outputs of its preceding dropout layer and the $(8 - i)^{th}$ conv layer/block. The input to the generator network is a 4-dimensional image. The first three dimensions are the RGB channels of the input image, and the 4th dimension is the the sensitivity parameter w. The structure of the generator is illustrated in Figure 3.

Architecture of the discriminator. The input to the discriminator is a pair of images, an RGB scene image and a shadow map image, which is either the ground-truth map or the map generated by the generator. Specifically the RGB image will be stacked with the mask to form the input with 4 channels. The output of the discriminator is a probability value for the image pair to be real, i.e., the shadow map is actually the shadow mask corresponding to the shadows in the scene image. The discriminator is a CNN with the following layers: conv_R64, conv_BR128, conv_BR256,
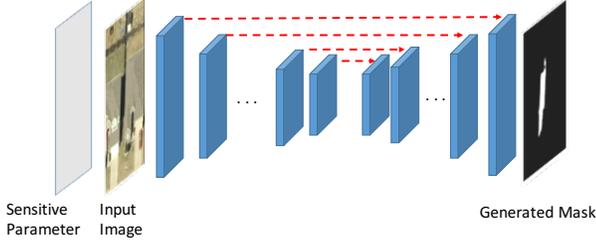
Figure 3: **Generator's architecture,** a U-Net [26] based encoder-decoder with skip connections similar to [6].
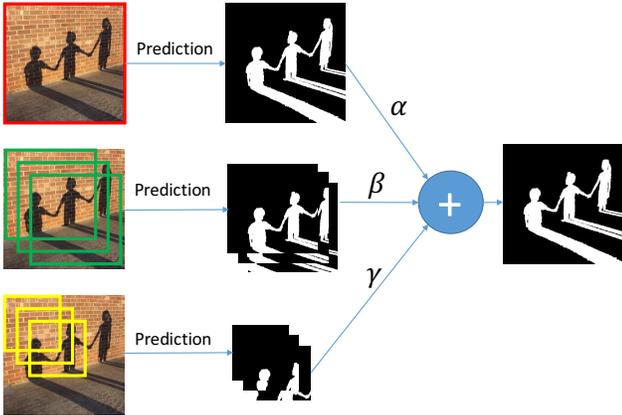
Figure 4: **Weighted aggregation scheme.** The final predicted shadow map for an image is the weighted average of shadow maps computed for multiple image patches at multiple locations and scales. On average, there are 280 overlapping patches per image, and $\alpha = 25, \beta = 5, \gamma = 1$.

conv_BR512, FC where conv_R denotes a convolutional layer followed by Leaky ReLU; conv_BR is a block of convolutional layer, batch normalization and Leaky ReLU; FC is a fully connected layer combined with a sigmoid activation function.

3.4. Training details

We train an scGAN with Stochastic Gradient Descent and the Adam solver [10], similar to [6]. One training iteration consists of performing one gradient step on D, followed by two gradient steps on G. This is to ensure that the loss of the discriminator does not reach zero. At each iteration, we pick an image and create a batch of multiple training instances from the image using data augmentation. This batch contains:

- The original image resized to 256×256 pixels.
- Patches $3/4$ the size of the original image, extracted with a stride of 20, down sampled to 256×256.
- 256×256 patches of the original image, sampled with a stride of 20.

Using the above procedure, we obtain an average of 13 training instances from each original training image. At every training iteration, each instance is trained with a new value of w sampled from $\mathcal{U}[0, 1]$. We train our scGAN from scratch. We initialize all the weights of the convolutional and deconvolutional layers of G and D by sampling from a zero-mean normal distribution with standard deviation 0.2. We set all the biases to 0.

3.5. Multi-scale shadow prediction

The shadow map for a given testing image is obtained as follows. From the image, we obtain overlapping image patches at multiple scales. Each image patch is resized to 256×256 and fed into the generator to obtain a 256×256 shadow map. The shadow maps are scaled back to the sizes of the corresponding patches, and multiple overlapping shadow maps are aggregated to create the shadow map for the testing image. The image patches obtained from the testing image at multiple scales are:

- s_1: The original testing image.
- s_2: Crops covering $3/4$ of the images, extracted with a stride of 20.
- s_3: 256×256 patches extracted with a stride of 20.

With that configuration, each testing image has 280 crops on average. The final predicted shadow map is the weighted average of the pixel predictions from all the resized shadow maps. The weights α, β, γ for the scales s_1, s_2, s_3 are 25, 5, and 1, respectively. Figure 4 depicts this prediction process.

4. Experiments and Results

To evaluate the shadow detection performance of our proposed method we perform experiments on the SBU Shadow dataset [30] and the UCF Shadow dataset [32]. These datasets contain input RGB images and their corresponding ground-truth binary shadow masks. The SBU dataset has 4089 training images and 638 testing images. It is the largest publicly available annotated shadow dataset. The UCF dataset consists of 221 images which are divided into training and testing sets in a similar way to [4]. To evaluate shadow detection performance quantitatively, we compare the provided ground-truth masks and the masks predicted by our method. As the main evaluation metric we use the balance error rate (BER):

$$\text{BER} = 1 - \frac{1}{2}\left(\frac{TP}{TP+FN} + \frac{TN}{TN+FP}\right) \quad (8)$$

BER is commonly used because of the unbalanced nature of shadow data: in natural images there are much fewer shadow pixels than non shadow pixels. We also compute separate per pixel error rates per class.

4.1. Shadow detection evaluation on SBU

We train our proposed scGAN on the SBU training set. We evaluate the shadow detection performance of the trained model on the SBU testing set. In Table 1, we compare our results with the stackedCNN, the state-of-the-art method on this dataset [30]. As can be seen, scGAN outperforms stackedCNN by a wide margin; in terms of BER we obtain a significant 17% error reduction. Moreover, scGAN effectively reduces the error in shadow pixels by 19% while also correctly detecting 17% more non shadow pixels than the stackedCNN. These are significant improvements over a datataset of almost 700 images depicting a wide variety of scene types.

Methods	BER	Shadow	Non Shad.
StackedCNN [30]	11.0	9.6	12.5
cGAN	13.6	20.5	**6.9**
scGAN (this paper)	**9.1**	**7.8**	10.4

Table 1: **Evaluation of shadow detection on SBU Shadow dataset [30]**. Testing results on SBU test subset for methods training on SBU train subset. Performance measured by Balance Error Rate(BER) and per class error rate. Our proposed method achieves around 17% error reduction across metrics with respect to the previous state of the art StackedCNN [30]. Best results printed in bold.

In Fig. 5, we contrast qualitatively the performance of scGAN and stackedCNN [30]. Compared to stackedCNN we can observe how scGAN is not as easily fooled by the local appearance of the dark albedo surfaces such as the bolt, the tombstone, the blackboard and the clothing from the scenes depicted in the first four rows. Our proposed method is also more precise in detecting shadows cast on brighter materials such as the snow scene in the fifth row. We show additional qualitative examples for challenging scenes in Figure 7. These images present some filter/lens effects, locally ambiguous appearance, and poor illumination conditions, respectively.

4.2. Shadow detection evaluation on UCF

We also evaluate our method for the cross-dataset shadow detection task. In this experiment, we evaluate the proposed scGAN model trained on the SBU training set for shadow detection, on the UCF testing set [32]. This a very challenging task as the SBU training set does not overlap with the UCF data sets. In Table 2, we compare to stackedCNN [30], the state of the art method for the cross dataset task on UCF. We conducted two experiments, one with the model trained from UCF-Training, the other from SBU-Training. In both experiments, we achieved better results with 6% decrease of BER in the UCF-trained model

and 12% decrease of BER in the SBU-trained model. Remarkably, the scGAN trained on SBU obtains better testing performance in UCF, compared to the stackedCNN method actually trained on the UCF training set itself.

Method	Training Set	BER	Shadow	Non Shad.
stackedCNN [30]	UCF-Train	11.6	10.4	12.6
scGAN (proposed)	UCF-Train	**10.9**	10.4	11.4
stackedCNN [30]	SBU-Train	13.0	9.0	17.1
scGAN (proposed)	SBU-Train	**11.5**	**7.7**	15.3

Table 2: **Comparison of shadow detection results on UCF testing set.** In terms of BER, our proposed method outperforms state of the art stackedCNN[30] by 6% and 12%, when training with UCF-Training and SBU-Training respectively.

4.3. Effects of Sensitivity Parameters

To illustrate the effects of the sensitivity parameter w in the proposed scGAN method, we evaluate shadow detection performance on the SBU testing set [30] for different values of w. As shown in Table 3, testing with higher values of w effectively increases the sensitivity of the trained models towards shadow pixels (minority class). In terms of Balance Error Rate (BER), the scGAN model achieves best performance for $w = 0.7$.

w	BER	Shadow	Non Shad.
0.3	10.6	15.4	5.8
0.5	9.7	12.4	7.0
0.7	**9.0**	**8.7**	**9.4**
0.8	9.1	7.8	10.4
0.9	10.6	4.7	16.5

Table 3: **Influence of the sensitivity parameter in shadow detection**. The proposed scGAN model is trained on SBU Shadow dataset [30], testing with different values of sensitivity parameter w. Performance measured by BER and per class error rate on SBU testing set. Shadow error rate decreases when the sensitivity parameter increases. The best overall performance is achieved for 0.7.

4.4. scGAN vs cGAN

We compare the proposed scGAN with a cGAN model of our architecture on the SBU dataset. The cGAN version is obtained by setting λ as zero in the objective function, hence training without any data loss term. Shadow detection results with the cGAN deteriorate considerably when testing in SBU. The BER drops to 13.6 which is a 49% decrease compared to scGAN. This demonstrates the benefits

(a) Input Image   (b) Ground-truth Mask   (c) stackedCNN [30]   (d) scGAN(ours)
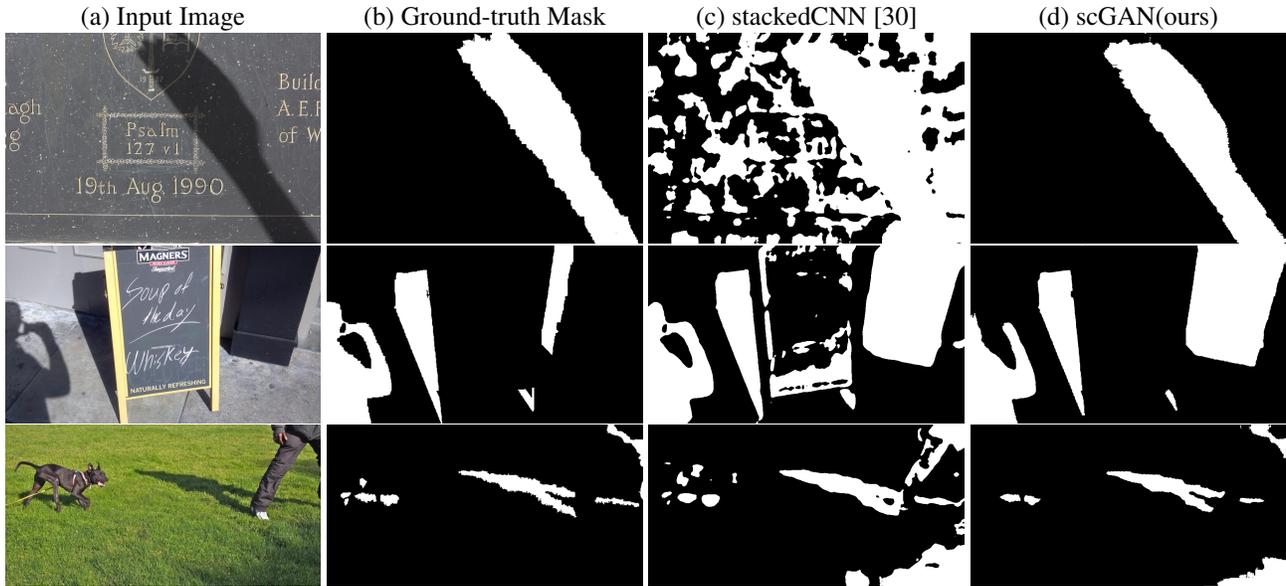
Figure 5: **Comparison of shadow detection on SBU dataset.** (a) Input image. (b) Shadow ground-truth mask. (c) Predicted mask by the stackedCNN[30]. (d) Predicted mask by our proposed method scGAN.

of our proposed approach. In Figure 6, we show qualitative comparisons of scGAN and cGAN. In the 2nd row of Table 1, we can see that, unsurprisingly, cGAN prefers to classify more non-shadow pixels correctly than shadow pixels (which is by far the smallest class).

5. Conclusions

In this paper, we have formulated the shadow detection problem in a generative adversarial framework. We have shown how to parameterize the loss function to handle severely unbalanced training sets without needing to train multiple models for tuning. Our method significantly reduced errors when tested on the most challenging available shadow datasets. The proposed method can also be applied on other classification problems with unbalanced classes such as infrastructure inspection problems (e.g., road surface condition datasets).

References

[1] G. Finlayson, M. Drew, and C. Lu. Entropy minimization for shadow removal. *International Journal of Computer Vision*, 2009.

[2] G. Finlayson, S. Hordley, C. Lu, and M. Drew. On the removal of shadows from images. *IEEE Transactions on Pattern Analysis and Machine Intelligence*, 2006.

(a) Input Image   (b) cGAN   (c) scGAN
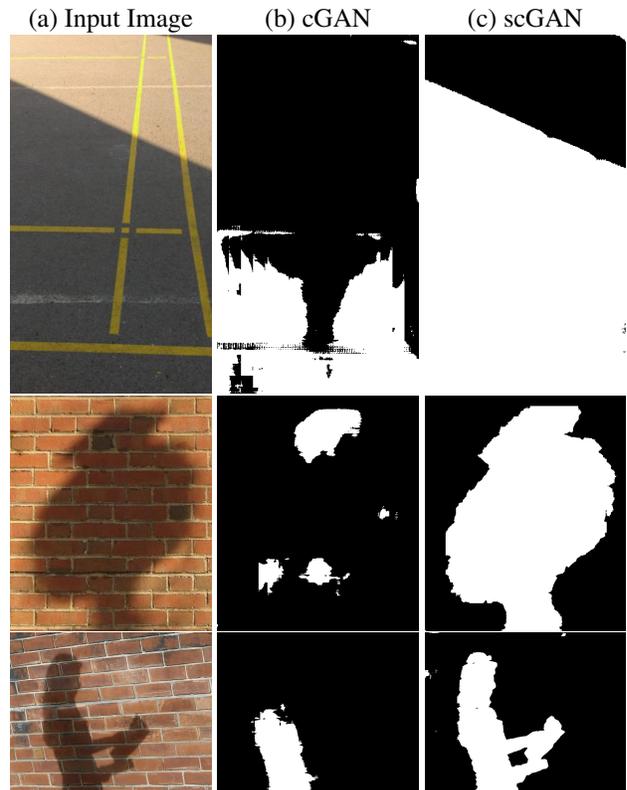
Figure 6: **Detection results scGAN vs cGAN.** (a) Input image. (b) cGAN prediction. (c) scGAN prediction.

[3] I. J. Goodfellow, J. Pouget-Abadie, M. Mirza, B. Xu,

(a) Input Image   (b) Ground-truth Mask   (c) Predicted Mask
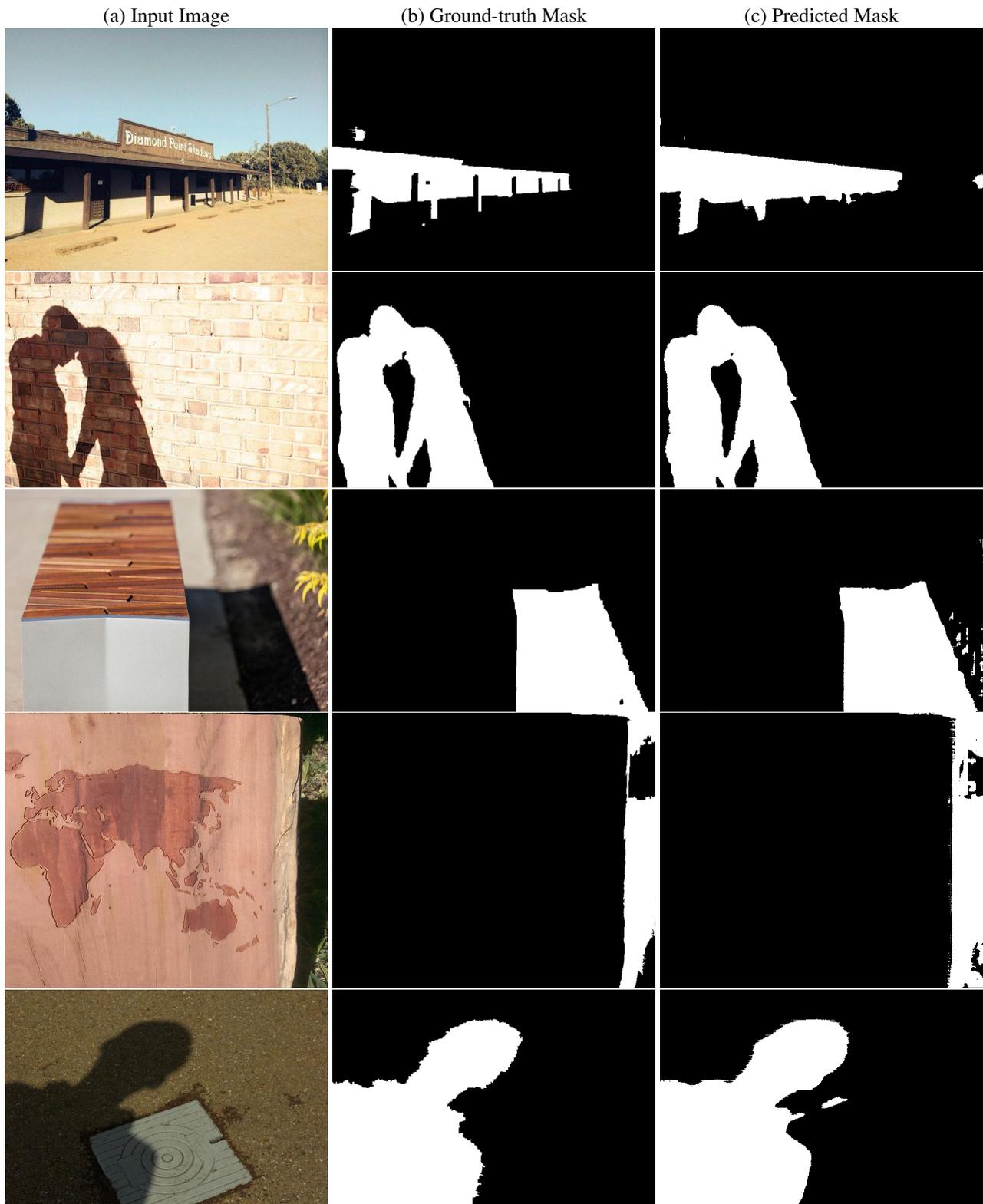
Figure 7: **Shadow detection examples on the SBU dataset.** (a) Input image. (b) Shadow ground-truth mask. (c) Predicted mask by our proposed method scGAN.

D. Warde-Farley, S. Ozair, A. C. Courville, and Y. Bengio. Generative adversarial networks. In *Advances in Neural Information Processing Systems*, 2014.

[4] R. Guo, Q. Dai, and D. Hoiem. Single-image shadow detection and removal using paired regions. In *Proceedings of the IEEE Conference on Computer Vision and Pattern Recognition*, 2011.

[5] X. Huang, G. Hua, J. Tumblin, and L. Williams. What characterizes a shadow boundary under the sun and sky? In *Proceedings of the International Conference on Computer Vision*, 2011.

[6] P. Isola, J. Zhu, T. Zhou, and A. A. Efros. Image-to-image translation with conditional adversarial networks. In *Proceedings of the IEEE Conference on Computer Vision and Pattern Recognition*, 2017.

[7] I. Junejo and H. Foroosh. Estimating geo-temporal location of stationary cameras using shadow trajectories. In *Proceedings of the European Conference on Computer Vision*, 2008.

[8] K. Karsch, V. Hedau, D. Forsyth, and D. Hoiem. Rendering synthetic objects into legacy photographs. *ACM Transactions on Graphics*, 2011.

[9] H. Khan, M. Bennamoun, F. Sohel, and R. Togneri. Automatic feature learning for robust shadow detection. In *Proceedings of the IEEE Conference on Computer Vision and Pattern Recognition*, 2014.

[10] D. P. Kingma and J. Ba. Adam: A method for stochastic optimization. In *Proceedings of the International Conference on Learning Representations*, 2015.

[11] J. D. Lafferty, A. McCallum, and F. C. N. Pereira. Conditional random fields: Probabilistic models for segmenting and labeling sequence data. In *Proceedings of the International Conference on Machine Learning*, 2001.

[12] J.-F. Lalonde, A. Efros, and S. Narasimhan. Estimating natural illumination from a single outdoor image. In *Proceedings of the European Conference on Computer Vision*, 2009.

[13] J.-F. Lalonde, A. A. Efros, and S. G. Narasimhan. Detecting ground shadows in outdoor consumer photographs. In *Proceedings of the European Conference on Computer Vision*, 2010.

[14] Y. LeCun, B. Boser, J. S. Denker, and D. Henderson. Backpropagation applied to handwritten zip code recognition. *Neural Computation*, 1(4):541–551, 1989.

[15] C. Ledig, L. Theis, F. Huszr, J. Caballero, A. Cunningham, A. Acosta, A. Aitken, A. Tejani, J. Totz, Z. Wang, and W. Shi. Photo-realistic single image super-resolution using a generative adversarial network. In *Proceedings of the IEEE Conference on Computer Vision and Pattern Recognition*, 2017.

[16] C. Li and M. Wand. Precomputed real-time texture synthesis with markovian generative adversarial networks. In *Proceedings of the European Conference on Computer Vision*, 2016.

[17] J. Long, E. Shelhamer, and T. Darrell. Fully convolutional networks for semantic segmentation. In *Proceedings of the IEEE Conference on Computer Vision and Pattern Recognition*, 2015.

[18] P. Luc, C. Couprie, S. Chintala, and J. Verbeek. Semantic segmentation using adversarial networks. In *NIPS Workshop on Adversarial Training*, 2016.

[19] C. C. M. Mathieu and Y. LeCun. Deep multi-scale video prediction beyond mean square error. In *Proceedings of the International Conference on Learning Representations*, 2016.

[20] M. Mirza and S. Osindero. Conditional generative adversarial nets. In *NIPS Deep Learning and Representation Learning Workshop*, 2014.

[21] S. I. Okabe, T and Y. Sato. Attached shadow coding: estimating surface normals from shadows under unknown reflectance and lighting conditions. In *Proceedings of the European Conference on Computer Vision*, 2009.

[22] A. Panagopoulos, D. Samaras, and N. Paragios. Robust shadow and illumination estimation using a mixture model. In *Proceedings of the IEEE Conference on Computer Vision and Pattern Recognition*, 2009.

[23] A. Panagopoulos, C. Wang, D. Samaras, and N. Paragios. Illumination estimation and cast shadow detection through a higher-order graphical model. In *Proceedings of the IEEE Conference on Computer Vision and Pattern Recognition*, 2011.

[24] A. Panagopoulos, C. Wang, D. Samaras, and N. Paragios. Simultaneous cast shadows, illumination and geometry inference using hypergraphs. *IEEE Transactions on Pattern Analysis and Machine Intelligence*, 2013.

[25] D. Pathak, P. Krähenbühl, J. Donahue, T. Darrell, and A. Efros. Context encoders: Feature learning by inpainting. In *Proceedings of the IEEE Conference on Computer Vision and Pattern Recognition*, 2016.

[26] O. Ronneberger, P.Fischer, and T. Brox. U-net: Convolutional networks for biomedical image segmentation. In *Medical Image Computing and Computer-Assisted Intervention (MICCAI)*, 2015.

[27] T. F. Y. Vicente, M. Hoai, and D. Samaras. Leave-one-out kernel optimization for shadow detection. In *Proceedings of the International Conference on Computer Vision*, 2015.

[28] T. F. Y. Vicente, M. Hoai, and D. Samaras. Noisy label recovery for shadow detection in unfamiliar domains. In *Proceedings of IEEE Conference on Computer Vision and Pattern Recognition*, 2016.

[29] T. F. Y. Vicente, M. Hoai, and D. Samaras. Leave-one-out kernel optimization for shadow detection and removal. *IEEE Transactions on Pattern Analysis and Machine Intelligence*, 2017.

[30] T. F. Y. Vicente, L. Hou, C.-P. Yu, M. Hoai, and D. Samaras. Large-scale training of shadow detectors with noisily-annotated shadow examples. In *Proceedings of the European Conference on Computer Vision*, 2016.

[31] Y. Zhou and T. L. Berg. Learning temporal transformations from time-lapse videos. In *Proceedings of the European Conference on Computer Vision*, 2016.

[32] J. Zhu, K. Samuel, S. Masood, and M. Tappen. Learning to recognize shadows in monochromatic natural images. In *Proceedings of the IEEE Conference on Computer Vision and Pattern Recognition*, 2010.